Synthesis of bioadditives of fuels from biodiesel-derived glycerol by esterification with acetic acid on solid catalysts

Gabriel A. Bedogni, Mauro D. Acevedo, Federico Aguzín, Nora B. Okulik & Cristina L. Padró

Taylor & Francis
Taylor & Francis Group

Check for updates

Synthesis of bioadditives of fuels from biodiesel-derived glycerol by esterification with acetic acid on solid catalysts

Gabriel A. Bedogni[a], Mauro D. Acevedo[b], Federico Aguzín[a], Nora B. Okulik [a] and Cristina L. Padró[b]

[a]Universidad Nacional del Chaco Austral, Pcia. Roque Sáenz Peña, Chaco, Argentina; [b]Catalysis Science and Engineering Research Group (GICIC), Instituto de Investigaciones en Catálisis y Petroquímica -INCAPE-(UNL-CONICET), Santa Fe, Argentina

ABSTRACT

In this paper, glycerol esterification with acetic acid (AA) was studied on several solid acid catalysts: Al_2O_3, Al-MCM-41, HPA/SiO_2, HBEA, Amberlyst 15 and Amberlyst 36 with the aim of determining the reaction conditions and the nature of the surface acid sites required to produce selectively triacetylglycerol (triacetin). The acidity of the catalysts (nature, density and strength of acid sites) was characterized by temperature-programmed desorption of NH_3 and FTIR of adsorbed pyridine. Al_2O_3 (Lewis acidity) did not show any activity in the reaction. In contrast, highest activity and selectivity to the triacetylated product (triacetin) were obtained on catalysts with Brønsted acidity: Amberlyst 15 and Amberlyst 36. The effect of temperature and molar ratio of AA to glycerol was studied, and the results showed that both parameters have a significant impact on the production of the desired product. Glycerol conversion rate and selectivity to triacetin increased when temperature or AA to glycerol molar ratio were increased, reaching a triacetin yield on Amberlyst 36 of 44% at 393 K and AA to glycerol molar ratio of 6. Deactivation and reusability of Amberlyst 36 were evaluated by performing consecutive catalytic tests. The presence of some irreversible deactivation due to sulfur loss was observed. In addition, the feasibility of using crude glycerol from biodiesel production as reactant was also investigated. Conversion of crude pretreated glycerol yielded values of triacetin and diacetin similar to those obtained with the commercial pure glycerol although at a lower rate.

1. Introduction

On the last years, global biodiesel market has shown a significant increase, expecting to reach 37 billion gallons by 2016 [1–3]. Argentina has had a sustained increase in biodiesel production so that it has been among the top five countries for several years. In 2011, with a production of 2100 million liters reached third place behind Germany and Brazil. However due to constrained export markets in 2015, the production suffered a fall and occupied the fourth place behind the U.S., Brazil and Germany [4].

Biodiesel is generally produced by (trans)esterification of natural oils and the main by-product is glycerol, which is formed in significant amounts (10wt.%) [5]. In consequence, the glycerol production has grown and a considerable drop in the price has been observed, leading to interest in finding new routes to valuable chemicals from this by-product [6–9].

In general, the conversion of glycerol may be divided into two classes: (i) oxidation, reduction or dehydration of glycerol into other three carbon compounds; (ii) reaction with other molecules (esterification, condensation, polymerization or etherification).

Although the price of pure glycerol (PG) is between two and four times higher than the crude glycerol (CG) price, the direct conversion of CG into derivatives has been rarely reported [1,10,11]. The main drawback of using CG from biodiesel is the content of impurities such as methanol, water, matter organic non-glycerol (MONG), mainly composed by soaps and free fatty acids (FFAs) [12–14], and alkali metal ions from KOH or NaOH, used as catalysts for (trans)esterification process.

The use of CG has been studied in propylene glycol, acrolein and dihydroxyacetone synthesis and also in H_2 production, finding that the activity of the solid catalysts employed is affected by the presence of impurities such as FFA and salts [15–18]. However, these products can still be synthesized and therefore more investigation to improve the processes is encouraged.

Esterification of glycerol leads to the formation of valuable products used as additives for food, pharmaceuticals and biofuels. The product obtained and the
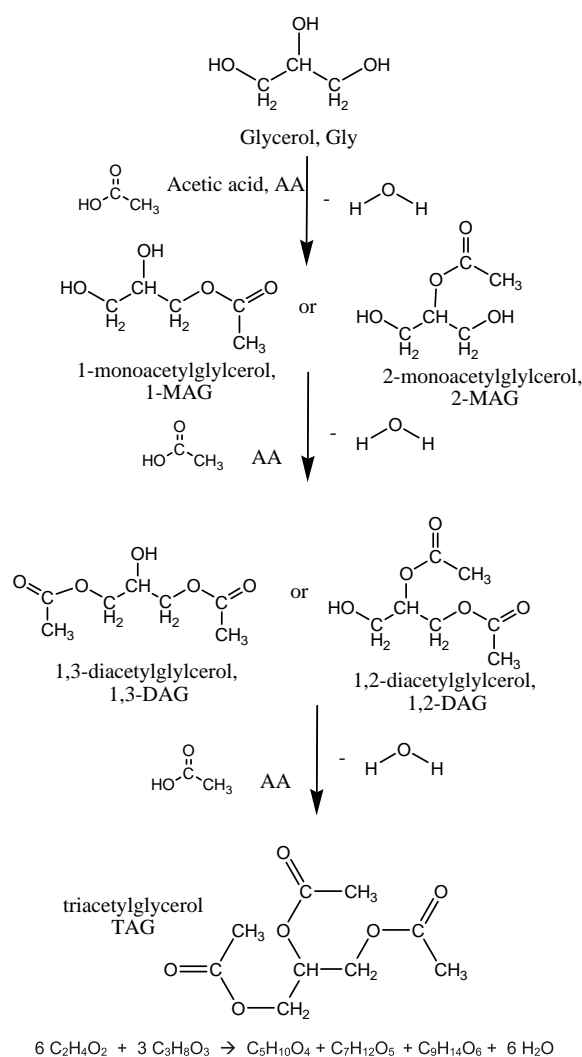
Scheme 1. Reaction of esterification of glycerol with AA.

subsequent use thereof depend on the chemical nature of the other reactant: acetic anhydride [19], lauric acid [20], etc. Esterification with acetic acid (AA) or anhydride provides a series of compounds: mono-acetylglycerols (monoacetins, 1-MAG and 2-MAG), di-acetylglycerols (diacetins, 1,2-DAG and 1,3 DAG) and triacetylglycerol (triacetin, TAG), as shown in the reaction (Scheme 1). MAG and DAG are used in cryogenic liquids and especially as starting materials for the production of biodegradable polyesters [21]. TAG has applications ranging from cosmetics to fuel additives [22]. As additive, TAG improves various fuel properties that could be particularly useful for improving the quality of the biodiesel from which glycerol is the main by-product [23]. In fact, many researchers have found that TAG addition [23,24] results in a final fuel having enhanced cold and viscosity properties. Garcia et al. [25] also have demonstrated that TAG not only improves effectively the fuel viscosity but also allows it to meet the specification in EN14214 [26]

and ASTM D6751 [27] standards for flash point and oxidation stability.

Commercial processes involving esterification in most cases use liquid acid catalysts and high temperatures pose environmental concerns due to the generation of a significant amount of harmful effluents and wastes. Therefore, the development of alternative environmentally friendly processes is especially encouraged. The replacement of the liquid acid by solid acid catalysts such as zeolites, commercial resins, functionalized mesostructured solids, carbon-based catalysts and supported dodecatungstophosphoric acid have been studied [28–33].

Goncalves et al. [28] have tested in glycerol acetylation Amberlyst 15, niobic acid and zeolites HZSM5 and HUSY using an AA/glycerol ratio of 3, under reflux. On Amberlyst 15, which presented the highest activity, the maximum selectivity to TAG obtained was 13% for a glycerol conversion of 97%. The acid strength of the sulfonic acid sites has been mentioned as a determinant parameter in the catalytic performance of SBA-15 functionalized catalysts. In fact, catalysts functionalized with arenesulfonic acid and fluorosulfonic acid showed higher selectivity to DAG and TAG than the functionalized with propyl sulfonic acid [29]. Other authors have reported the use of carbon as a support [30,31], which has the advantage of being stable at high temperature and easily functionalized. However, the reusability of these materials is limited by the leaching of the active compounds in polar liquids.

High selectivity to TAG was reached using acetic anhydride as an acylating agent [19,34], but this compound has higher cost and is more aggressive than AA.

Despite the publication of many papers about glycerol acetylation, there is only one work [22] that reported the use of CG in this reaction, indicating a good catalytic performance although no data of impurities content or glycerol source were informed.

In this paper, we have studied the glycerol esterification with AA on solid acids with the aim to determine the reaction conditions and the nature of the surface acid sites required to selectively produce TAG. In addition, we have analyzed the feasibility of using CG from biodiesel production as reactant in this reaction.

2. Experimental

2.1. Materials

The following is a list of the materials' purity and source/supplier: glycerol (Cicarelli, 98%), AA (Cicarelli, 99.5%), sodium silicate (Aldrich, 14% NaOH, 27% SiO_2), aluminum isopropoxide (Aldrich, 98+%), cetyltrimethylammonium

bromide (CTABr, Sigma-Aldrich, ≥98%), Al_2O_3 (CK-300 Cyanamid Ketjen), HBEA (Zeocat PB, Si/Al = 25), HPA (H_3-$PW_{12}O_{40}.6H_2O$, Sigma-Aldrich R.G.), SiO_2 (Davisil Grade 62 Sigma-Aldrich), Amberlyst 15 and Amberlyst 36 Wet (Rohm & Haas), Triacetin (Sigma-Aldrich, >99%) and Methanol (Merck, >99%).

2.2. Catalysts preparation

Commercial resins Amberlyst 15 and Amberlyst 36 Wet were pretreated at 353 K in an oven during 4 h before use.

The mesoporous solid Al-MCM-41 was prepared by sol–gel method, according to Edler and White [35]. The reagents used in this work were: sodium silicate and aluminum isopropoxide as source of silicon and aluminum respectively, cetyltrimethylammonium bromide as surfactant and distilled water (molar gel composition: $7SiO_2$–$0.2Al_2O_3$–$2.7Na_2O$–$3.7CTABr$–$1000H_2O$). The gel was heated in a Teflon-lined stainless steel autoclave at 373 K during four days. After crystallization, the solid was filtered, washed with distilled water, dried in oven at 373 K and finally calcined in air at 773 K for 6 h. More information about Al-MCM-41 synthesis is informed in Supplementary Information. Commercial Al_2O_3 and HBEA were calcined at 723 K in flowing air before use.

2.3. Impregnation of catalyst

HPA/SiO_2 was supported on SiO_2 by incipient wetness impregnation [36,37] using 2 ml/g of HPA aqueous solution at room temperature. In order to determine the impregnation volume, 1.5 g of SiO_2 was dried in an oven at 393 K for 4 h. Then deionized water was added dropwise until reaching the desired wetting point, which was achieved with 3.1 ml of water. Impregnated silica was dried at 393 K and then treated at 523 K in flowing N_2 during 3 h in a glass reactor.

2.4. Characterizations of catalyst

BET surface areas (S_g), mean pore diameter ($\overline{d_p}$) and pore size distribution were measured by N_2 physisorption at 77 K in a Quantachrome instrument model autosorb-1C sorptometer. The crystalline structure of Al-MCM-41 was determined by X-ray diffraction (XRD) using a Shimadzu XD-D1 diffractometer and Ni-filtered Cu Kα radiation. Density and strength of surface acid sites were studied by temperature-programmed desorption (TPD) of NH_3. Samples were treated in He (60 cm^3/min) at 773 K for 2 hours. The adsorption of NH_3 was carried out at 373 K using a 1%NH_3–99%He mixture. Weakly adsorbed NH_3 was removed by flushing with He at 373 K for 90

minutes. Temperature was then increased at 10 K/min and the NH_3 concentration in the effluent was measured by mass spectrometry in a Baltzers Omnistar unit.

The nature of surface acid sites of catalysts was determined by infrared (IR) spectroscopy by using pyridine as probe molecule and a Shimadzu Prestige-21 spectrophotometer according to a procedure detailed in [38]. The catalysts were ground to a fine powder and pressed into wafers (10–30 mg). The discs were mounted in a quartz sample holder inside of a Pyrex cell equipped with CaF_2 windows. The samples were outgassed in vacuum at 723 K (due to the low thermal stability, HPA/SiO_2 was treated at 573 K) during 2 hours and cooled to 298 K under evacuation. Spectra were recorded at room temperature, after admission of pyridine, adsorption at room temperature and sequential evacuation at 298, 423 and 573 K.

Sulfur content of the catalyst was analyzed by energy dispersive X-ray fluorescence spectroscopy using a Shimadzu EDX720 system.

2.5. CG treatment and analysis

The CG (pH = 9.11) was supplied by a local biodiesel plant in Chaco, Argentina, which used sunflower oil as the raw material and NaOH as catalyst. Prior to use, part of this CG was pretreated, selecting a low-cost procedure that does not involve the formation of a large amount of waste. The refining process of CG to purified crude glycerol (PCG) involved three stages: (i) removal of FFA and salt by acidification to pH 2.5 with H_3PO_4 (85 wt.%), centrifugation, to separate the three phases, neutralization of glycerol containing phase (middle layer) with NaOH 0.0125M solution and subsequent centrifugation to eliminate the salts formed; (ii) removal of methanol and water: by evaporation at 378 K and solvent extraction with ethanol (to ensure the salts' precipitation) and (iii) deep refining by activated carbon adsorption at 373 K.

Analysis of crude and purified glycerol was made as follows: (i) methanol and free acids were determined by GC analysis using a HP 6890 equipped with a HP5 column and a FID detector; (ii) moisture content was determined by Karl Fisher titrator SI Analytics model TitroLine Alpha 20 Plus, and (iii) phosphorus, potassium and sodium content was analyzed by energy dispersive X-ray fluorescence spectroscopy using a Shimadzu EDX720 system.

2.6. Catalytic activity

Liquid phase glycerol esterification with AA was carried out in a stainless steel batch reactor (Parr 4560). In a typical experiment, the reactor was loaded with 20 g of

glycerol (Gly) and 1 g of catalyst, then was flushed with N_2 to eliminate the air. The temperature in the reactor was raised up to 353 K, and 78.3 g of AA was incorporated (AA:Gly molar ratio 6:1). The mixture was heated to the reaction temperature and maintained constant for 4 hours (total reaction time). The reactor pressure was kept at 392 kPa by using N_2 as inert gas.

Samples were collected periodically, filtered and refrigerated (in order to stop the reaction), then analyzed and quantified using a HP 7820A (Agilent Technologies) gas chromatograph equipped with a FID detector and a capillary column Agilent J&W HP-5 (length 30 m, diameter 0.32 mm and film thickness 0.25 μm) and EZCrome Elite software. The column temperature was initially set at 398 K followed by a ramp of 5 K/min to 433 K according to the procedure reported by Nebel et al. [39] to analyze the acetylglycerols mixture. Reaction products (MAG, DAG and TAG) were identified by using gas chromatography mass spectrometry (Thermo Scientific ISQEISM) and pure compounds. Response factors of glycerol and TAG were experimentally determined while the remaining factors were estimated theoretically (see Supplementary Information).

Glycerol conversion (X_{Gly}) and product selectivities (S_i) were calculated as: $X_{Gly} = \sum C_i / \sum (C_i + C_{Gly})$ and $S_i = C_i / \sum C_i$, where C_i are the concentration of products from glycerol and C_{Gly} is the glycerol concentration.

In order to determine the effect of AA:glycerol molar ratio (AA:Gly), additional experiments at 373 K were performed using three different reactant proportions: 4:1, 6:1 and 8:1. The influence of the temperature on the glycerol acetylation was determined using a AA:Gly ratio of 6. The selected temperatures for this research were 333, 353 and 373 K. These experiments were carried out using Amberlyst 15 as catalysts.

The loss of catalytic activity of the resin Amberlyst 36 was studied by performing a run at 353 K and AA:Gly ratio of 6 during 120 minutes until the glycerol concentration drops by 80% with respect to the initial value (corresponding to $X_{Gly} = 80\%$), then 16 g of glycerol was

rapidly loaded without opening the reactor and the reaction was followed for 120 minutes.

The reusability of the resin Amberlyst 36 was evaluated at 353 K by carrying out four consecutive catalytic runs with the same sample. After each experiment, the catalyst was separated by filtration, washed with warm water (303 K) to remove the remaining products and reactants, dried at 353 K in an oven and reutilized in the following catalytic run.

3. Results and discussion

3.1. Catalyst characterization

The results of surface area determined by N_2 physisorption are shown in Table 1. The incorporation of bulky HPA molecules caused a decrease in the surface area of SiO_2 from 300 m²/g (SiO_2) to 205 m²/g by blocking mainly the micropores, increasing the mean pore diameter from 150 Å (SiO_2) to 223 Å. XRD pattern of Al-MCM-41(not shown here) exhibits a strong diffraction peak at 2.2° and two small peaks at 3.7° and 4.3° corresponding to 100, 110 and 200 reflections, respectively, indicating that the sample is well crystallized. The surface area and pore diameter values determined by N_2 physisorption of this sample are in good agreement with values reported previously [35,40].

The acidity of the catalysts was studied by TPD of NH_3 preadsorbed at 373 K and IR of pyridine. The densities of surface acid sites (mmol/g) were obtained by deconvolution and integration of TPD traces (TPD curves are not shown here) and they are presented in Table 1. The values reported for Amberlyst 15 and Amberlyst 36 were provided by their manufacturer, because their poor thermal stability does not allow the TPD procedure. Al_2O_3 and Al-MCM-41 have very low density of acid sites followed by HPA/SiO_2. Amberlyst 36 presents the highest density of acid sites according to the manufacturer data (Table 1) while Amberlyst 15 has a density of acid sites slightly lower than the other resin.

Table 1. Physical properties and acidity of the samples used in this work.

Catalyst	Pore size (Å)	S_g (m²/g)	Acidity (mmol/g)	FTIR of pyridine $T_{desorption} = 423$ K Brønsted sites (area/g)	Lewis sites (area/g)	$T_{desorption} = 573$ K Brønsted sites (area/g)	Lewis sites (area/g)
Amberlyst 15	300[a]	45[a]	4.7[a]	–	–	–	–
Amberlyst 36 Wet	240[a]	33[a]	5.4[a]	–	–	–	–
HPA/SiO_2	223	205	0.16	169	74	116[b]	8[b]
HBEA	6.7	560	0.78	150	151	74	92
Al-MCM-41	30	935	0.21	14	54	2	52
Al_2O_3		230	0.17	0	114	0	69

[a]Manufacturer datasheet.
[b]Desorption temperature: 523 K.

The chemical nature and strength of surface acid sites were investigated by analyzing the FTIR spectra obtained after adsorption of pyridine at 298 K and evacuation at 423 and 573 K (Figure SI3). Pyridine adsorbed on Brønsted acid sites shows absorption bands at 1540, 1480–1500 and 1640 cm^{-1} [41,42]. Pyridine coordinately bonded on Lewis acid sites produces characteristic bands at 1440–1460, 1480–1500 and 1600 cm^{-1}. The relative contributions of Lewis and Brønsted acid sites after evacuation of pyridine at 423 and 573 K were obtained by deconvolution and integration of the bands at 1445–1455 cm^{-1} (Lewis) and 1540 cm^{-1} (Brønsted); results are given in Table 1. Al$_2$O$_3$ presented essentially Lewis acidity; the band at 1540 cm^{-1} was not observed. FTIR spectra of zeolite HBEA and Al-MCM-41 after desorption at 423 K showed the contribution of both Lewis and Brønsted acid sites, but, while HBEA presented similar concentration of both type of sites, the Brønsted-to-Lewis ratio is almost 0.25 for Al-MCM-41. HPA/SiO$_2$ presented mainly Brønsted acidity; after sample evacuation at 423 and 523 K Brønsted-to-Lewis ratios were 2.4 and 14.5, respectively. It is important to remark that Brønsted acid sites of this catalysts are strong, retaining after evacuation at 523 K almost 70% of the pyridine adsorbed after evacuation at 423 K. The presence of Lewis acid sites on HPA/SiO$_2$ has been reported previously [43] and has been attributed to the presence of two species at HPA loadings 20% or lower: HPA retaining the Keggin structure, and a lacunary or unsaturated specie of Lewis acid character formed by interaction with the silica support [44].

3.2. Catalytic activity results

In all the catalytic experiments, the products observed were the mono, di and triacetylated glycerols. Despite reported by other authors [28], no products from glycerol dehydration (acetol or acrolein) were detected. Among the monoacetylated glycerols, the isomer substituted in the terminal carbon (1-MAG) was predominant, giving rise to a 1-MAG/2-MAG molar ratio between 7 and 9. Regarding the diacetylated glycerols, the 1,3-DAG/1,2-DAG molar ratio was close to 2. Dosuna et al. [45] have also identified and analyzed the isomers monoacetylated and diacetylated (MAG and DAG); and they have reported a similar tendency. In a previous paper [46], we have studied this reaction, both experimentally and theoretically, finding that external OH are easier to attack, leading to an esterification on the primary carbon atom. The values determined by theoretical studies are consistent with those found experimentally and show that 1-MAG is the prevailing monoester and 1,3-DAG is the prevailing diester. Therefore, the transformation of glycerol into 1-MAG and then into 1,3-DAG to produce TAG would be the appropriate path for the reaction.

In the rest of this work, selectivities to both mono-acetins (1-MAG, and 2-MAG) are informed as S_{MAG} and selectivities to diacetins (1,2-DAG, and 1,3 DAG) as S_{DAG}, without further differentiation.

In order to select temperature and AA to glycerol molar ratio for further comparison of all the catalyst, we have studied the influence of these variables on catalytic activity and selectivity using Amberlyst 15 as catalyst. We have chosen a resin for this test since their high activity in esterification reactions has been reported [28,45,47].

3.2.1. Effect of reaction temperature

The effect of the temperature on the glycerol esterification reaction was investigated using an AA to glycerol molar ratio of 6. Glycerol conversion and product selectivities as a function of reaction time for three different temperatures (333, 353 and 373 K) are plotted in Figure 1.

The glycerol conversion increased with time, showing different rates; at 333 K the conversion after 4 hours of reaction was still increasing while at 373 K the highest value of glycerol conversion was reached in the first hour. As expected, the glycerol conversion rates at time zero (r^0_{Gly}) (calculated from the initial slope of C_{GLY} vs. time curves) grew up from 3.1 mmol/g min at 333 K, to 5.6 at 353 K and finally to 17.4 mmol/g min at 373 K, indicating the significant effect of this parameter.

Regarding the product distribution, a remarkable change in selectivity curves was observed. The selectivity to the primary product (MAG) showed a maximum more pronounced and at lower time as the temperature was increased; S_{DAG} only presented a maximum at 373 K at about 60 minutes when the selectivity value was higher than 60%. Formation of TAG was significant only at 373 K, reaching a value of 19.7% at final time. The raise in selectivity towards secondary and tertiary products (DAG and TAG) with the reaction temperature may simply be due to the increase in the conversion and the consequent displacement of the reaction to these products, or may additionally exist a preferential increase of the corresponding rate constant (higher activation energy). In fact, it could be observed at 373 K, few minutes after the reaction was started, when the conversion reached a value close to 30% the selectivities were $S_{MAG} = 76\%$, $S_{DAG} = 22\%$, $S_{TAG} = 2\%$, values for diacetylated and triacetylated higher than those achieved at lower temperatures even at higher values of conversion. This variation in product selectivity cannot be explained only by a change in glycerol conversion, probably
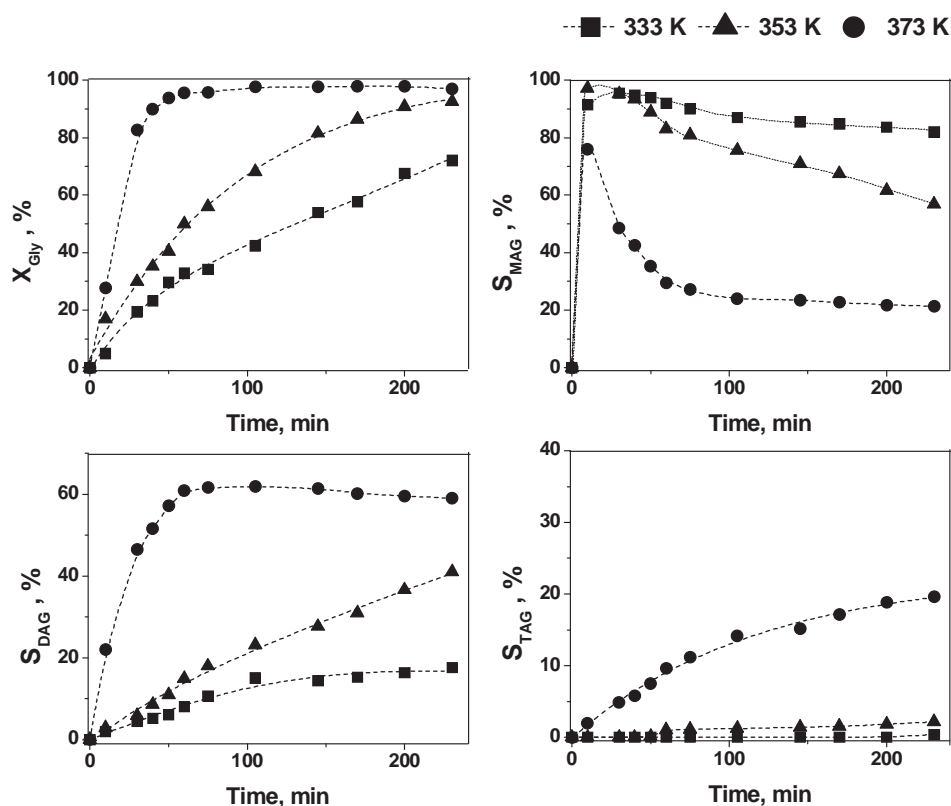
Figure 1. Conversion of glycerol and selectivity at 333 K (■), 353 K (▲) and 373 K (●), catalyst: Amberlyst 15, catalyst concentration 5.53 g/l, molar ratio 6:1 (AA/Gly) and stirring speed: 800 rpm.

showing a high value of activation energy for the step of TAG formation as it has been suggested previously [48]. This is also highlighted in the literature by several authors [49,50], who have also pointed out that the consecutive acetylation reactions are endothermic, particularly the MAG to DAG step, which could explain the elevated MAG formation at lower temperatures.

3.2.2. Effect of AA to glycerol molar ratio

There is a discrepancy about this topic in literature; while several authors have reported a raise in the glycerol conversion with the increase in AA/Gly molar ratio and consequently in the secondary and tertiary products formation (DAG and TAG) [19,51], other authors have claimed that an increase in the AA:Gly molar ratio has the opposite effect, a diminution in glycerol conversion and selectivities to DAG and TAG [52]. Lastly, Kayhoon et al. [53] have found that the increase in molar ratio has a positive effect on conversion up to AA/Gly = 8; higher values of AA/Gly molar ratio did not produce any change.

In order to study the influence of the reactants' molar ratio on glycerol conversion and product selectivities, the AA/glycerol molar ratio was varied from 4 to 8. Amberlyst 15 was used as catalyst and the reaction temperature was 373 K. Glycerol conversion and initial

glycerol conversion rate (r_{GLY}^0) are shown in Figure 2(A). Even though AA:Gly ratio was varied from 4 to 8, little change in final conversion was observed. On the other hand, by raising the AA/Gly molar ratio from 4 to 6, the AA concentration is increased and a positive effect on the glycerol conversion rate was observed, denoting that kinetics of the reaction depends on this parameter. However, a further increase caused a decline in r_{GLY}^0 value, passing through a maximum for a molar ratio of 6. The diminution in the conversion rate is probably due to the strong adsorption of AA on the acid sites of the catalyst, thereby decreasing the accessibility of glycerol [45] or just by a dilution effect of glycerol.

With the aim of analyzing the effect of the molar ratios in the distribution of reaction products, in Figure 2(B,C), selectivities at 100 and 240 minutes are plotted. In order to study only the influence of the molar ratio, t = 100 min was chosen to compare selectivities because at this time the glycerol conversion in these three reactions have reached a similar value of about 90%. In Figure 2(B), an increase in the selectivity to secondary and tertiary products (DAG and TAG) is observed when the molar ratio is increased, at expenses of MAG selectivity, even for the molar ratio of 8, despite the decrease in the initial rate of conversion of glycerol observed in this
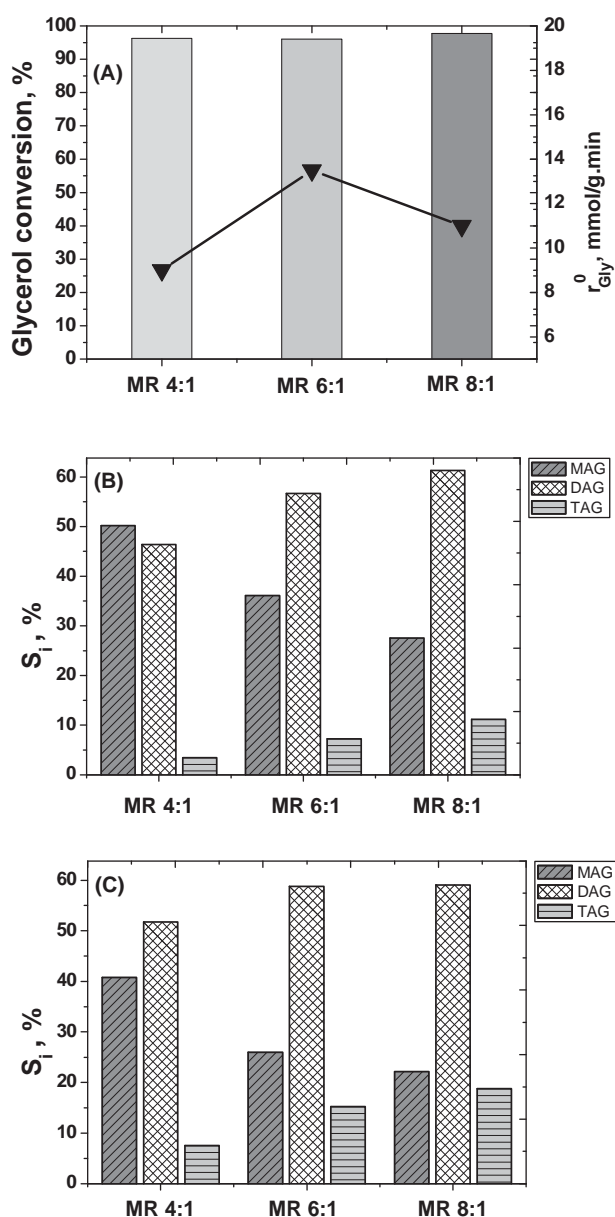
Figure 2. Glycerol conversion (X_{Gly}) at 240 min and initial glycerol conversion rate (r^0_{Gly}), ▼. (A) Products selectivities (S_i) at 100 min (B) and 240 min (C) at different molar ratios, $T =$ 373 K, catalyst: Amberlyst 15, catalyst concentration 5.53 g/l and stirring speed: 800 rpm.

conditions. Since AA is also reactant in secondary and tertiary esterification reactions (MAG → DAG and DAG → TAG), all the reaction rates involved could depend on this reactant; thus higher AA concentrations promote these reactions, leading to the formation of DAG and TAG products. At 240 min (Figure 2(C)), S_{TAG} reached 19% when the AA/Gly molar ratio used was 8, while selectivity to DAG grew up from 52% to 59% when ratio was increased from 4 to 6; however, further increase in this ratio did not modify the value of this selectivity.

3.2.3. Catalysts' evaluation

Based on the results shown above, the conditions selected to compare the catalysts include: a temperature of 373 K and a AA:Gly molar ratio of 6:1. The conversions and selectivities values obtained at 240 minutes for all the catalysts used in this work are given in Table 2. Glycerol conversion rates at time zero (r^0_{Gly}) were calculated as the initial slope of C_{GLY} vs. time curves and are also included in Table 2.

The results obtained on Al_2O_3 are practically identical to the results without solid catalyst (Blank), demonstrating that Lewis acid sites present on this catalyst are not suitable to promote the glycerol esterification although the use of homogeneous Lewis acid catalyst, $SnCl_2$, as efficient catalyst has been previously reported [54].

The acid resins have been claimed to be efficient catalysts for esterification reactions [47], particularly Amberlyst 15 and Amberlyst 35 have exhibited higher activity than zeolites in the glycerol acetylation [19,28]. In this work, highest initial glycerol conversion rates and final glycerol conversions were obtained on Amberlyst 15 ($X_{GLY} = 97.1\%$, $r^0_{Gly} = 17.4$ mmol/g min) and Amberlyst 36 ($X_{GLY} = 93.1\%$, $r^0_{Gly} = 12.8$ mmol/g min), which in turn have the highest densities of acid sites.

HPA/SiO_2, which has lower density of acid sites (mainly Strong Brønsted) than HBEA (similar contribution of Lewis and Brønsted acidity), presented higher glycerol conversion than the zeolite probably due to the presence of strong Brønsted acid sites or less diffusion constraint. Al-MCM-41 showed similar initial glycerol conversion rate than HBEA, although its acid site density is almost four times lower, thereby indicating that the mesoporosity of this material increases the accessibility of reactants to the acid sites.

In Table 2, we have also included the initial rate of glycerol conversion per mmol of acid site, calculated dividing the initial conversion rate per gram (r^0_{Gly}, mmol/g min)

Table 2. Catalytic results for the liquid phase esterification of glycerol with AA.

Catalyst	r^0_{Gly} (mmol/ g min)	r^0_{Gly} (mmol/ mmol min)	X_{Gly} (%)	S_{MAG} (%)	S_{DAG} (%)	S_{TAG} (%)
Amberlyst 15	17.4	3.7	97.1	21.2	59.1	19.7
Amberlyst 36	12.8	2.4	93.1	26.0	58.8	15.2
Amberlyst 36[a]	18.8	3.5	98.8	7.0	48.9	44.1
HPA/SiO₂	2.6	10.9	87.0	85.1	14.4	0.5
HBEA	1.7	1.15	66.8	73.0	25.8	1.2
Al-MCM-41	1.5	3.3	52.8	80.4	18.8	0.8
Al₂O₃	0.8	0.5	33.4	88.8	10.9	0.3
Blank	0.8	–	32.5	89.5	10.5	0

Note: Reaction conditions: temperature 373 K, molar ratio 6:1 (AA/Gly), stirring speed: 800 rpm, catalyst concentration: 5.53 g/l and reaction time 240 minutes.
[a]Temperature 393 K, molar ratio 6:1 (AA/Gly), stirring speed: 800 rpm, catalyst concentration: 5.53 g/l and reaction time 240 minutes.
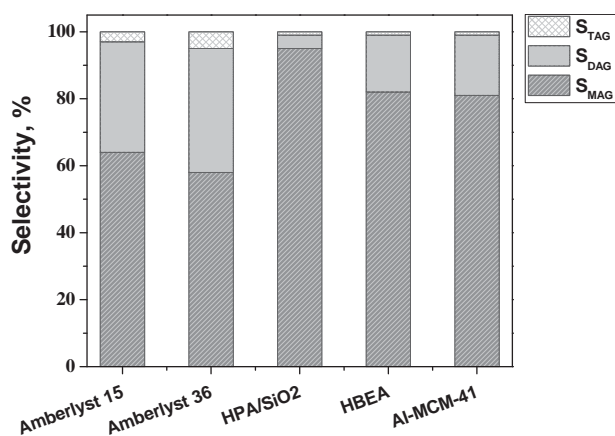
Figure 3. Selectivities at $X_{GLY} = 50\%$ (glycerol conversion) (373 K catalyst concentration 5.53 g/l, molar ratio 6:1 (AA/Gly) and stirring speed: 800 rpm).

after subtracting the value of blank (r^0_{Blank}, mmol/g min), by the density of acid sites (Table 1). HPA/SiO$_2$ shows the highest value (10.9 mmol/mmol min) followed by Amberlyst 15, suggesting that strong Brønsted acid sites are very active for esterification of glycerol. However, HPA/SiO$_2$ formed very little of secondary and tertiary product at 240 min ($S_{DAG} = 14.4\%$ and TAG was detected only in trace amount). By contrast, Amberlyst 15 was more selective to TAG (tertiary product formed by consecutive esterification reactions), reaching a value of 19.7% at 240 minutes under the reaction conditions.

In order to get more insight about the role of the catalyst in product distribution, we have plotted in Figure 3 the selectivities at same value of glycerol conversion ($X_{GLY} = 50\%$). On HPA/SiO$_2$, the selectivity to di- and triacetylated products ($S_{DAG} + S_{TAG}$) is less than 5%, while on HBEA and Al-MCM-41 is almost 20%. Ferreira et al. have tested catalyst based on HPA supported on SiO$_2$ [55] or carbon [56] in this reaction under more severe conditions ($T = 393$ K and AA/glycerol molar ratio = 16). They have also reported low selectivity to secondary and tertiary products, although they have not compared with other catalysts. One of the remarkable characteristics of solid HPA is the ability of absorption of large quantity of polar or basic molecules such as alcohols and nitrogen bases in the solid bulk [57]. Alcohols can desorb easily, but other compounds require high temperature to leave. The strong absorption of glycerol or the esters could be the cause of this different behavior [54].

On the other hand, the high selectivities to intermediate and final (DAG and TAG) products on the resins are clearly shown in Figure 3. Amberlyst 36, the most selective catalyst, forms 40% of secondary and tertiary product, with a selectivity to TAG of 5% at this level of conversion ($X_{GLY} = 50\%$). Both commercial resins have

the same nature of the acid sites (–SO$_3$H$^+$ groups), but Amberlyst 36 poses higher superficial density of sites than Amberlyst 15 (0.16 and 0.10 mmol/m^2) and smaller pore size that could favor the consecutive reactions to form triacetin.

Due to the significantly good catalytic performance of the resins, particularly for obtaining secondary and tertiary products, Amberlyst 36, which has higher thermal stability than Amberlyst 15 (maximum operation temperature of Amberlyst 15 and 36: 393 and 423 K, respectively), was tested a 393 K in the reaction, keeping all other conditions (AA/Gly molar ratio 6:1, stirring speed: 800 rpm, catalyst concentration: 5.53 g/l). The initial rate of glycerol conversion per millimole of acid site on Amberlyst 36 increased from 2.4 at 373 K to 3.5 at 393 K (Table 2). As it was previously demonstrated (Figure 1), selectivities to secondary and tertiary products (DAG and TAG) are significantly affected by the reaction temperature. Selectivity to TAG on Amberlyst 36 at 393 K reached a value of 44% at final time, which means 43.6% of yield, making this catalyst the most promising for triacetylated glycerol obtaining.

3.2.4. Catalyst deactivation

With the aim of studying the activity decay of the catalyst (Amberlyst 36), we have carried out two consecutive catalytic tests without stopping the reaction according to the following procedure: after 120 minutes of run (reaction conditions: 373 K, AA:Gly 6:1), we loaded in the reactor 16 g of glycerol (in order to have the same initial amount of reactant). The glycerol concentration was plotted as a function of reaction time in Figure 4. It is noted that the slope of the second curve is somewhat smaller than the first and the glycerol
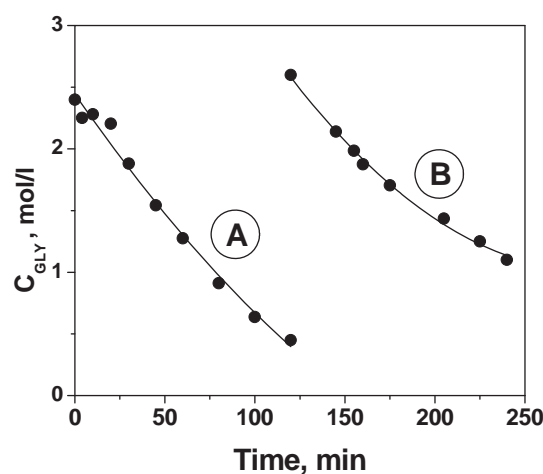

Figure 4. (A) Glycerol injection and (B) Glycerol reinjection, molar ratio 6:1 (AA/Gly), $T = 373$ K, catalyst: Amberlyst 36 (catalyst concentration 5.53 g/l) and stirring speed: 800 rpm.

concentration in the second cycle is slightly greater, indicating that although part of the active acid sites on the catalyst surface have been lost, most of them remain available during the reaction. We have calculated the initial glycerol conversion rate at time zero and immediately after the glycerol reinjection and the loss in the rate was 14%, suggesting the presence of some deactivation of the catalyst. This activity loss could be produced by both the presence of strongly adsorbed high molecular weight products on active sites (reversible or partially reversible deactivation), strong adsorption of water that prevents the adsorption of reactants [45] or loss of active sites either by sintering, pore blockage or release of sulfonic acid groups (acid sites of resins). If the deactivation is provoked by adsorption or deposition of heavy compounds, catalytic activity can be recovered by removing deposits from the catalyst by washing with a solvent that solubilize them. In contrast, the sulfonic group loss is an irreversible phenomenon.

3.2.5. Catalyst reusability test

The reusability of catalyst Amberlyst 36 was evaluated as follow: four consecutive runs were performed at same reaction conditions (373 K, AA:Gly 6:1) using the same sample of Amberlyst 36. Between reactions, the catalyst was washed with warm water and dried overnight at 353 K. In the literature, the resins' reusability studies showed different results: Testa et al. [52] have reported that Amberlyst 15 activity decreases after the third reuse cycle, obtaining a glycerol conversion of only 60% in the fifth cycle; therefore, selectivity to MAG increases
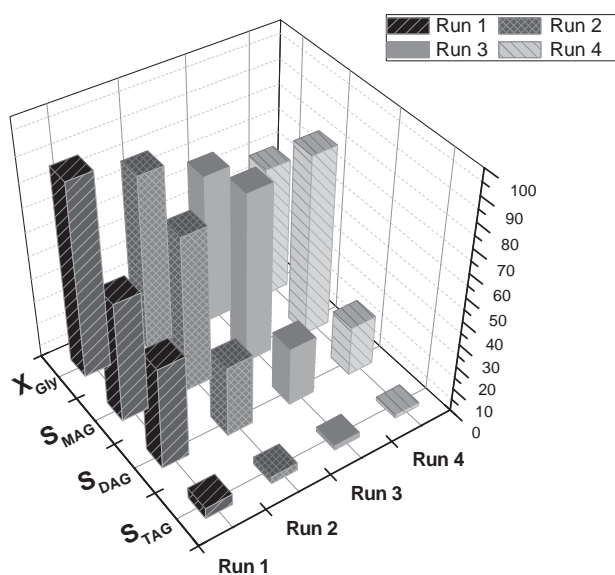
at the expense of DAG and TAG. Other authors have carried out reusability test using Amberlyst 36 and Dowex-2 [45] but using glycerol excess. They have obtained unexpected higher yield of esters (sum of the three isomers) in second cycle compared with the first run, which was attributed to desorption of product from the catalyst that was not washed between reactions.

Results of our experiments as glycerol conversion and product selectivity at 120 minutes of reaction are shown in Figure 5. The drop in glycerol conversion between the first and fourth run was 32%, but the changes in selectivities were greater, selectivity to the primary product (S_{MAG}) increased from 51% to 77% because of the lost in activity, while selectivity to secondary (S_{DAG}) and tertiary products (S_{TAG}) decreased 43% and 67%, respectively. A decrease in the activity from the first to the fourth run was observed denoting that the washing of the catalyst did not make possible to recover active sites (Table 3). Since this result could be indicating the degradation of the resin, even though the catalytic tests were performed at temperature lower than the maximum operation temperature of this material, the Sulfur content of the catalyst was analyzed after first and fourth run. Results are included in Table 4. Sulfur content of fresh catalyst is included for comparison. The loss of Sulfur, and therefore of active catalytic sites, was about 3% after the first run and rise to 25.5% after four consecutive catalytic runs, demonstrating the presence of some degradation of this resin under the reaction condition used in this paper.

Figure 5. Catalyst reuse, molar ratio 6:1 (AA/Gly), $T = 373$ K, catalyst: Amberlyst 36 (catalyst concentration 5.53 g/l) reaction time 120 min and stirring speed: 800 rpm.

Table 3. Catalyst reusability test.

Catalytic run	r^0_{Gly} (mmol/g min)
First	4.5
Second	3.5
Third	2.7
Fourth	1.9

Note: Reaction conditions: molar ratio 6:1 (AA/Gly), $T = 353$ K, catalyst: Amberlyst 36 (catalyst concentration 5.53 g/l) and stirring speed: 800 rpm.

Table 4. Sulfur content of used catalysts.

	Sulfur content (wt.%)
Fresh	20
After first run	19.4
After fourth run	14.9

Note: Reaction conditions: molar ratio 6:1 (AA/Gly), $T = 353$ K, catalyst: Amberlyst 36 (catalyst concentration 5.53 g/l) and stirring speed: 800 rpm.

Table 5. CG and PCG composition.

	CG (wt.%)	PCG (wt.%)
Methanol	13.3	–
MONG	49.1	2.2
Humidity	1.4	2.0
Impurities and salts	3.7	1.0
Glycerol	32.5	94.8

3.2.6. Catalytic esterification of CG with AA

The composition of CG is shown in Table 5. The quality of CG depends on manufacturing biodiesel process and raw material used. The CG used in this work came from a process that use sunflower oil as raw material and NaOH as catalyst. The content of MONG mainly composed by
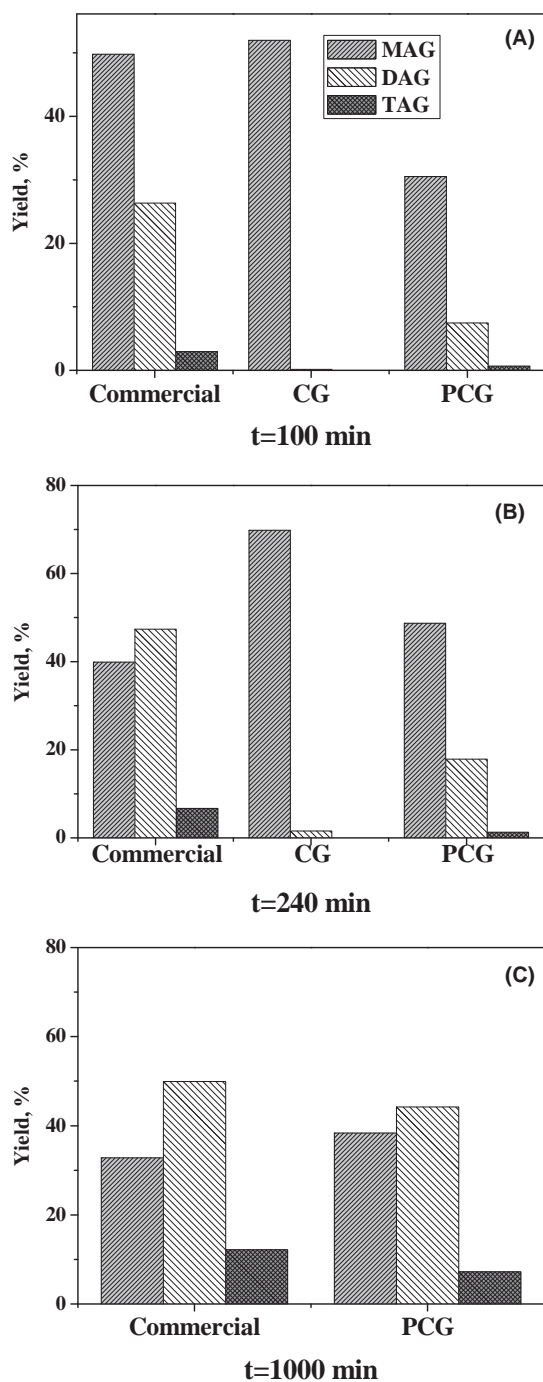
Table 6. Salts content in CG and PCG.

	Sodium ppm	Phosphorus ppm	Potassium ppm
CG	17,708	30.4	107
PCG	6567	3654	577

soaps and FFA is quite high, although similar to reported in previous papers [58,59]. Rehman et al. [59] have considered necessary to perform a pretreatment with the aim of eliminating the soaps and reducing the total organic fraction before using the CG in chemical process. They have lowered the pH by adding increasing amounts of H_3PO_4. We have conducted a similar pretreatment by acidification, and also solvent extraction and activated carbon adsorption. Glycerol treated (PCG) has a substantially lower content of MONG and methanol as displayed in Table 5. We have studied the effect of the impurities of glycerol from biodiesel production in direct conversion to acetylglycerols by carrying out the reaction using CG as raw material and comparing with the results using the pure commercial glycerol and crude glycerol purified in our lab (PCG). For these experiments, Amberlyst 36, which has good catalytic performance, was used as catalyst (reaction conditions: $T = 373$ K, AA/Gly molar ratio 6:1, stirring speed: 800 rpm, catalyst concentration: 5.53 g/l). The results after 100, 240 and 1000 minutes of reaction are exhibited in Figure 6 as MAG, DAG and TAG yield. It can be observed that MAG was formed almost exclusively when using CG even at 240 min. In addition, in this experiment, we observed formation of some solids evidencing the low feasibility of using glycerol as received from biodiesel plant. However, the pretreated glycerol (PCG) was transformed to DAG, and even to TAG reaching similar values to those obtained with the commercial glycerol although at a lower rate. This decrease in the activity could be due to some organic compound deposition on catalytic active sites or some exchange of H^+ by alkali cations (Na^+ and K^+). The content of this elements (Sodium and Potassium), besides phosphorus, is informed in Table 6.

Figure 6. MAG, DAG and TAG yields at 100 min (A), 240 min (B) and 1000 min (C) obtained with commercial glycerol, CG and PCG. Reaction conditions: molar ratio 6:1 (AA/Gly), $T = 373$ K, catalyst: Amberlyst 36 (catalyst concentration 5.53 g/l and stirring speed: 800 rpm).

4. Conclusions

Solid acids efficiently promote the esterification of glycerol with AA. Catalyst activity depends on the strength, density and nature of acid sites. Thereby, while Lewis acid sites are not suitable to catalyze the reaction, highest activity and selectivity to the triacetylated product (triacetin) were obtained on catalysts with Brønsted acidity: Amberlyst 15 and Amberlyst 36. However, on strong Brønsted acid sites present in HPA/SiO_2, even though highest glycerol conversion rate per acid site was achieved on this catalyst, very little of secondary and tertiary product was formed.

The effect of temperature and molar ratio of AA to glycerol was studied using Amberlyst 15 as catalyst. Both glycerol conversion rate and selectivity to triacetin increased when temperature or AA to glycerol molar ratio were increased, suggesting that the rates of the reactions from glycerol to triacetin depend on these parameters. The temperature has a remarkable impact on triacetin selectivity. An additional experiment using Amberlyst 36 (higher thermal stability than Amberlyst 15) at 393 K was performed; selectivity to desired product (TAG) of 44% was achieved at 240 minutes of reaction, being the highest value obtained in this work.

Deactivation and reusability of the catalyst were evaluated by performing consecutive catalytic tests with the same sample. A similar decrease in the initial activity was observed for both experiments that demonstrate the impossibility to recover the lost active sites by washing the catalyst between the catalytic runs performed for reusability test. A possible degradation of the resin is suggested by these results and confirmed by Sulfur analysis; loss of Sulfur, and therefore of active catalytic sites, was about 25.5% after four consecutive catalytic runs, proving the presence of some irreversible deactivation of this material under the reaction condition used in this paper.

Finally, we have studied the feasibility of direct conversion of CG or crude pretreated glycerol (PCG) to the acetylglycerols. We have found that is necessary to pretreat the CG to eliminate impurities such as soaps and FFAs. Then, by using PCG as raw material, DAG and TAG yield values similar to those obtained with the commercial glycerol, were reached although at a lower rate, indicating that impurities still present in PCG affected the catalyst activity.

Disclosure statement

Funding

ORCID

Nora B. Okulik 🅳 http://orcid.org/0000-0001-7568-3393

References

[1] Kong PS, Aroua MK, Daud WMAW. Conversion of crude and pure glycerol into derivatives: a feasibility evaluation. Renew Sust Energ Rev. 2016;63:533–555.

[2] Quispe CAG, Coronado CJR, Carvalho Jr JA. Glycerol: production, consumption, prices, characterization and new trends in combustion. Renew Sust Energ Rev. 2013;27:475–493.

[3] Yang F, Hanna M, Sun R. Value-added uses for crude glycerol – a byproduct of biodiesel production. Biotechnol Biofuels. 2012;5:1–10.

[4] REN21. Renewables2016 Global status report. Paris: REN21Secretariat 2016. p. 21.

[5] da Silva GP, Mack M, Contiero J. Glycerol: a promising and abundant carbon source for industrial microbiology. J Biotechnol Adv. 2009;27:30–39.

[6] Johnson D, Taconi K. The glycerin glut: options for the value-added conversion of crude glycerol resulting from biodiesel production. Environ Prog. 2007;26:338–348.

[7] Corma A, Huber G, Sauvanaud L, et al. Biomass to chemicals: catalytic conversion of glycerol/water mixtures into acrolein, reaction network. J Catal. 2008;257:163–171.

[8] Corma A. Inorganic solid acids and their use in acid-catalyzed hydrocarbon reactions. Chem Rev. 1995;95:559–614.

[9] Luo X, Ge X, Cui S, et al. Value-added processing of crude glycerol into chemicals and polymers. Biores Tech. 2016;215:144–154.

[10] Ayoub M, Abdullah AZ. Critical review on the current scenario and significance of crude glycerol resulting from biodiesel industry towards more sustainable renewable energy industry. Renew Sustain Energy Rev. 2012;16:2671–2686.

[11] He QS, McNutt J, Yang J. Utilization of the residual glycerol from biodiesel production for renewable energy generation. Renew Sust Energ Rev. 2017;71:63–76.

[12] Katryniok B, Paul S, Dumeignil F. Recent developments in the field of catalytic dehydration of glycerol to acrolein. ACS Catal. 2013;3:1819–1834.

[13] Konaka A, Tago T, Yoshikawa T, et al. Conversion of biodiesel-derived crude glycerol into useful chemicals over a zirconia–iron oxide catalyst. Ind Eng Chem Res. 2013;52:15509–15515.

[14] Liu R, Lyu S, Wang T. Sustainable production of acrolein from biodiesel-derived crude glycerol over $H_3PW_{12}O_{40}$ supported on Cs-modified SBA-15. J Ind Eng Chem. 2016;37:354–360.

[15] Dou B, Rickett GL, Dupont V, et al. Steam reforming of crude glycerol with in situ CO_2 sorption. Bioresour Technol. 2010;101:2436–2442.

[16] Boga DA, Liu F, Bruijnincx PCA, et al. Aqueous-phase reforming of crude glycerol: effect of impurities on hydrogen production. Catal Sci Technol. 2016;6:134–143.

[17] Auttanat T, Jongpatiwut S, Rirksomboon T. Dehydroxylation of glycerol to propylene glycol over Cu-ZnO/Al2O3 catalyst: effect of feed purity. Int J Chem Mol Nucl Mater Metall Eng. 2012;6:297–300.

[18] Kijenski J, Migdal A, Osawaru O, et al. Method for processing the glycerol phase from transesterification of fatty acid triglycerols. European Patent; EP1860090 A1. 2007.

[19] Liao X, Zhu Y, Wang S-G, et al. Producing triacetylglycerol with glycerol by two steps: esterification and acetylation. Fuel Process Technol. 2009;90:988–993.

[20] Sakthivel A, Nakamura R, Komura K, et al. Esterification of glycerol by lauric acid over aluminium and zirconium containing mesoporous molecular sieves in supercritical carbon dioxide medium. J Supercrit Fluids. 2007;42:219–225.

[21] Fukumura TT, Seki YT, Kubo M, et al. Catalytic synthesis of glycerol monoacetate using a continuous expanded Bed column reactor packed with cation-exchange resin. Ind Eng Chem Res. 2009;48:1816–1823.

[22] Zhu S, Zhu Y, Gao X, et al. Production of bioadditives from glycerol esterification over zirconia supported heteropolyacids. Bioresource Technol. 2013;130:45–51.

[23] B. Delfort, G. Hillion, I. Durand. FR Patent 2866654. 2004.

[24] J. Delgado. SP Patent 2201894. 2002.

[25] Garcia E, Laca M, Perez E, et al. New class of acetal derived from glycerin as a biodiesel fuel component. Energy Fuel. 2008;22:4274–4280.

[26] European Standard EN 14214. Automotive fuels. Fatty acid methylesters (FAME) for diesel engines. Requir Test Method. 2003;1–13.

[27] American Society for Testing and Materials (ASTM) Standard D6751. Standard specification for biodiesel fuel blend stock (B100) for middle distillate fuels. 2001.

[28] Goncalves VLC, Pinto BP, Silva JC, et al. Acetylation of glycerol catalyzed by different solid acids. Catal Today. 2008;133–135:673–677.

[29] Melero J, van Grieken R, Morales G, et al. Acidic mesoporous silica for the acetylation of glycerol: synthesis of bioadditives to petrol fuel. Energy Fuel. 2007;21:1782–1791.

[30] Ferreira P, Fonseca IM, Ramos AM, et al. Esterification of glycerol with acetic acid over dodecamolybdophosphoric acid encaged in USY zeolite. Catal Commun. 2009;10:481–484.

[31] Tao ML, Guan HY, Wang XH, et al. Fabrication of sulfonated carbon catalyst from biomass waste and its use for glycerol esterification. Fuel Process Technol. 2015;138:355–360.

[32] Gao X, Zhu S, Yongwang Li Y. Graphene oxide as a facile solid acid catalyst for the production of bioadditives from glycerol esterification. Catal Commun. 2015;62:48–51.

[33] Doyle AM, Albayati TM, Abbas AS, et al. Biodiesel production by esterification of oleic acid over zeolite Y prepared from kaolin. Renew Energy. 2016;97:19–23.

[34] Silva LN, Gonçalves VLC, Mota CJA. Catalytic acetylation of glycerol with acetic anhydride. Catal Commun. 2010;11:1036–1039.

[35] Edler KJ, White JW. Further improvements in the long-range order of MCM-41 materials. Chem Mater. 1997;9:1226–1233.

[36] Lefebvre F. 31P MAS NMR study of H3PW12040 supported on silica: formation of (=Si0H2+)(H2PW12040-). J Chem Soc Chem Commun. 1992;10:756–757.

[37] Mastikhin V, Kulikov S, Nosov A, et al. 1H and 31P MAS NMR studies of solid heteropolyacids and H3PW12O40 supported on SiO2. J Mol Cat. 1990;60:65–70.

[38] Padró CL, Apesteguía CR. Gas-phase synthesis of hydroxyacetophenones by acylation of phenol with acetic acid. J Catal. 2004;226:308–320.

[39] Nebel B, Mittelbach M, Uray G. Determination of the composition of acetylglycerol mixtures by 1H NMR followed by GC investigation. Anal Chem. 2008;80:8712–8716.

[40] Janicke MT, Landry CC, Christiansen SC, et al. Aluminum incorporation and interfacial structures in MCM-41 mesoporous molecular sieves. J Am Chem Soc. 1998;120:6940–6951.

[41] Parry EP. An infrared study of pyridine adsorbed on acidic solids. Characterization of surface acidity. J Catal 1963;2:371–379.

[42] Knözinger H. Specific poisoning and characterization of catalytically active oxide surfaces. In: Eley DD, Pines H, Weisz PB, editors. Advances in catalysis. Amsterdam: Elsevier Science; 1976; 25:184–271.

[43] Díez VK, Apesteguía CR, Di Cosimo JI. Synthesis of ionones by cyclization of pseudoionone on solid acid catalysts. Catal Lett. 2008;123:213–219.

[44] Kozhevnikov IV, Kloetstra KR, Sinnema A, et al. Study of catalysts comprising heteropoly acid H3PW12O40 supported on MCM-41 molecular sieve and amorphous silica. J Mol Catal A-Chem. 1996;114:287–298.

[45] Dosuna-Rodríguez I, Gaigneaux EM. Glycerol acetylation catalysed by ion exchange resins. Catal Today. 2012;195:14–21.

[46] Bedogni GA, Padró CL, Okulik NB. A combined experimental and computational study of the esterification reaction of glycerol with acetic acid. J Mol Model. 2014;20:1–13.

[47] Peters TA, Benes NE, Holmen A, et al. Comparison of commercial solid acid catalysts for the esterification of acetic acid with butanol. Appl Catal. 2006;297:182–188.

[48] Liao X, Zhu Y, Wang S-G, et al. Theoretical elucidation of acetylating glycerol with acetic acid and acetic anhydride. Appl Catal B: Environ. 2010;94:64–70.

[49] Trejda M, Stawicka K, Adam MZ. New catalysts for biodiesel additives production. Appl Catal B: Environ. 2011;103:404–412.

[50] Khayoon MS, Hameed BH. Synthesis of hybrid SBA-15 functionalized with molybdophosphoric acid as efficient catalyst for glycerol esterification to fuel additives. Appl Catal A-Gen. 2012;433–434:152–161.

[51] Gonçalves CE, Laier LO, Cardoso AL, et al. Bioaddictive synthesis from H3PW12O40-catalyzed glycerol esterification with HOAc under mild reaction conditions. Fuel Process Technol. 2012;102:46–52.

[52] Testa ML, Parola V, Liotta L, et al. Screening of different solid acid catalysts for glycerol acetylation. J Mol Catal A-Chem. 2013;367:69–76.

[53] Khayoon MS, Hameed BH. Acetylation of glycerol to biofuel additives over sulfated activated carbon catalyst. Bioresour Technol. 2011;102:9229–9235.

[54] Silva MJ, Laier LO, Gonçalves CE. Novel esterification of glycerol catalysed by tin chloride (II): a recyclable and less corrosive process for production of Bio-additives. Catal Lett. 2011;141:1111–1117.

[55] Ferreira P, Fonseca I, Ramos A, et al. Glycerol acetylation over dodecatungstophosphoric acid immobilized into a silica matrix as catalyst. Appl Catal B: Environ. 2009;91:416–422.

[56] Ferreira P, Fonseca IM, Ramos AM, et al. Acetylation of glycerol over heteropolyacids supported on activated carbon. Catal Commun. 2011;12:573–576.

[57] Mizuno N, Misono M. Heterogeneous catalysis. Chem Rev. 1998;98:199–218.

[58] Hu S, Luo X, Wan C, et al. Characterization of crude glycerol from biodiesel plants. J Agric Food Chem. 2012;60:5915–5921.

[59] Rehman A, Wijesekara RGS, Nomura N, et al. Pre-treatment and utilization of raw glycerol from sunflower oil biodiesel for growth and 1,3-propanediol production by Clostridium butyricum. J Chem Technol Biotechnol. 2008;83:1072–1080.